Steady-state simulation of mono-valent ion distributions within a nanofluidic channel

Will Booth[*,1], Jarrod Schiffbauer[1], Josh Fernandez[2], Kathleen Kelly[3], Aaron Timperman[3] , Boyd Edwards[1]
[1]Physics Dept., [2]Chemical Engineering Dept., [3]Chemistry Dept., West Virginia University
*Corresponding author: 3288 University Ave, Apartment 402, Star City, WV 26506
wbooth@mix.wvu.edu

Abstract: The steady-state non-equilibrium distributions of two species of mono-valent ions around a charged nanofluidic channel have been examined. Large reservoirs were placed on either side of the nanoscale channel to simulate bulk concentration of ions in a fluid. Results show that the effect of the potential bias across the nanochannel yields a significant depletion zone of ion concentrations near the end of the nanochannel.

Keywords: nano capillary channel ion simulation

1. Introduction

Despite recent efforts, a qualitative description of the dynamics and steady-state distribution of ions around nanofluidic channels is lacking. There are theoretical models for ion transport around capillaries or through micro and nanochannels [1]; however few depart from equilibrium [2]. Of specific interest is the ion transport and fluid flow across nanocapillary membranes [3-5]. In this work, we have examined the steady state, non equilibrium (5V – 100V) distribution of ions across a single nanochannel.

The simulations consist of two large square reservoirs acting as sources of bulk ion concentrations within a fluid. The walls of the nanochannel as well as the walls containing the channel between the two reservoirs represent insulating surfaces that interact with the aqueous solution and become charged through dissociation of surface molecules.

Figure 1 is an image of geometry used for the simulation. It is color coded to indicate the boundary conditions used, which will be discussed below.

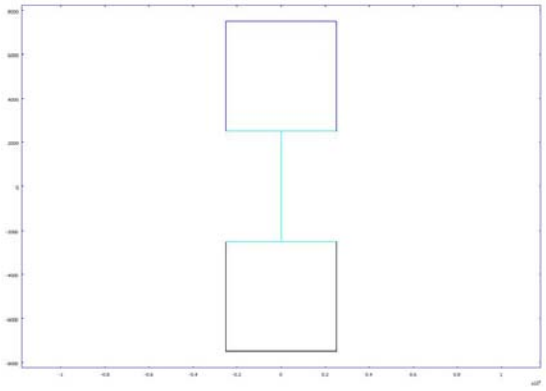

Figure 1. COMSOL Boundary Mode image of the simulation. The bottom walls in black are grounded. The nanochannel walls in light blue are insulated and set with a constant surface charge density. The top purple walls are biased from 5V-100V.

2. Theory

When the walls of the channel become charged, Coulombic forces attract opposite charges and repel like charges. This creates a layer of ions near the wall known as the Electric Double Layer. Unless dealing with narrow channels or low concentrations, the extent of the Stern layer is neglected. A diffuse layer of ions near the wall, with modified concentrations, is still produced though, due to the wall charge [6].

When an electric field pulls ions through a fluid the fluid can be dragged along with the ion flow [6]. There is still work to be done to determine whether or not the contribution of this electroosmotic flow, or EOF, is significant and to determine the ranges of concentrations or voltages for which it is significant [7]. EOF is neglected in these simulations.

The PNP (Poisson-Nernst-Planck) equations are used as the governing equations of the system. Poisson's equation is given by

$$\nabla^2\phi = -\frac{e}{\varepsilon}\left(n_+ - n_-\right) \tag{1}$$

Here ϕ is the electrostatic potential, $\varepsilon = 80\varepsilon_0$ is the permittivity, e is the electric charge, and n_i represents the ion concentration for $i = +,-$. The flux is given by the Nernst-Planck equation:

$$\vec{J}_i = -D_i\left(\vec{\nabla} n_i + \frac{en_i}{kT}\vec{\nabla}\phi\right) \tag{2}$$

Here D_i is the diffusion coefficient for each species and kT is the thermal energy. The continuity equation in the steady state then tells us the divergence of the flux is zero:

$$\vec{\nabla}\cdot\left(\vec{\nabla} n_i + \frac{en_i}{kT}\vec{\nabla}\phi\right) = 0 \tag{3}$$

The boundary condition for the charged walls of the nanochannel is given by

$$\frac{\partial\phi}{\partial n} = -\frac{\sigma}{\varepsilon} \tag{4}$$

where the derivative is with respect to the direction normal to the boundary and $\sigma = -10^{-3}\,C/m^2$ is the surface charge density set on the nanochannel walls.

The three walls of the lower reservoir are grounded, while the top three reservoir walls are set at 5V, 10V, and 100V. On each of these six reservoir walls, the concentration of each ion species was set to $n_b = 0.1mM$.

The COMSOL boundary conditions allow us to set the concentrations at bulk values on the reservoir walls while treating the nanochannel walls as insulating. This way there is no ion flux through the nanochannel walls while a flux is still yet allowed through the reservoir walls in order to keep bulk values.

The reservoirs were constructed to be $5\mu m$ squares. The nanochannel was $5\mu m$ long and $30nm$ wide.

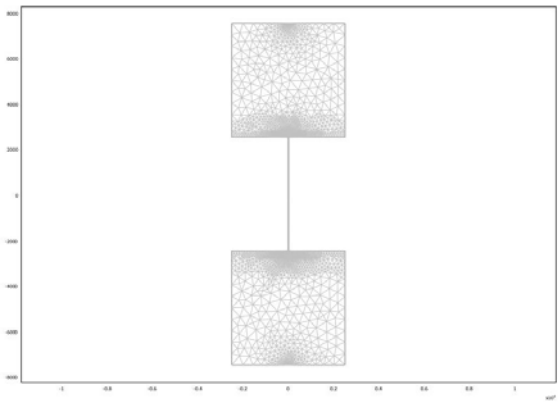

Figure 2. COMSOL mesh image used for the simulation.

3. Numerical Methods In COMSOL

Lagrangian quadratic elements were used with the DIRECT(UMFPACK) time independent solver in order to solve for the electrostatic potential and ion concentrations. A free meshing was used and refined largely around the nanochannel walls (figure 2).

The mesh was refined within and around the nanochannel due to the charged walls creating behavior which would not only deviate largely from bulk values but would also change significantly over small distances compared to the solutions in the reservoirs.

The Electrostatics module was used to model the electric potential. The Convection and Diffusion module was used twice, once for each ion species.

4. Results

The solutions in COMSOL Multiphysics yielded a depletion zone of both species of ions within the nanochannel on the side closest to the biased reservoir. Figures 3, 4 and 5 show a cross section down the middle of the length of the nanochannel of the ion concentrations for 5V, 10V, and 100V respectively.

We notice that the depletion zone extends about a quarter of the way inside the nanochannel for the 100V case. This gives evidence against the use of theoretical models which treat the channel as infinitely long and emphasizes the importance of end effects.

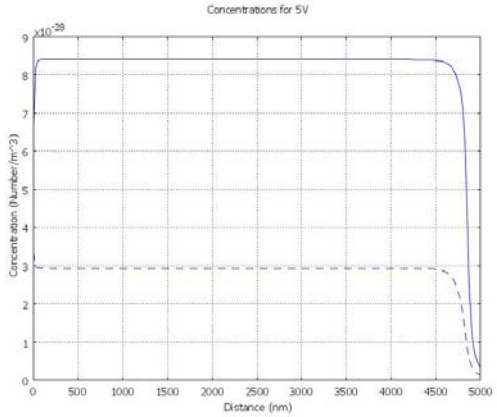

Figure 3. Cation concentration (solid trace) and anion concentration (dashed trace) vs. distance along the channel, for 5V applied across the nanochannel.

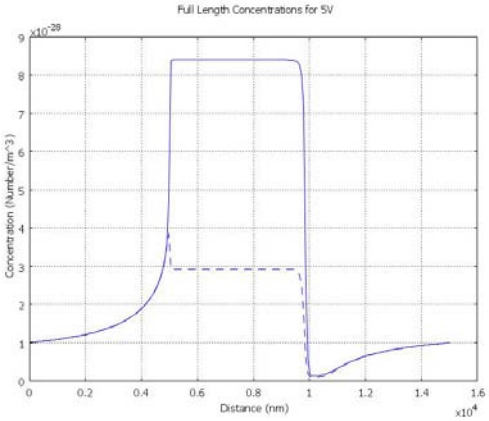

Figure 6. 5V applied. Cross sectional view of the ion concentrations. The left side is the grounded reservoir wall. The right side is the biased wall.

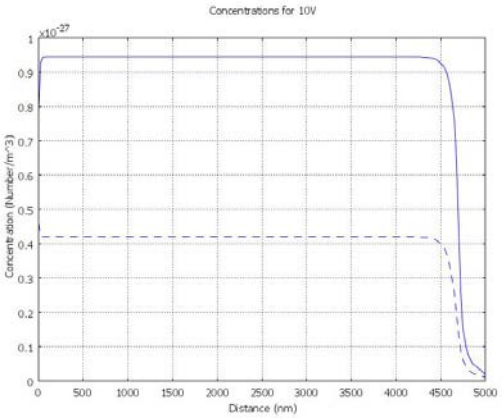

Figure 4. Concentrations with 10V applied across the nanochannel.

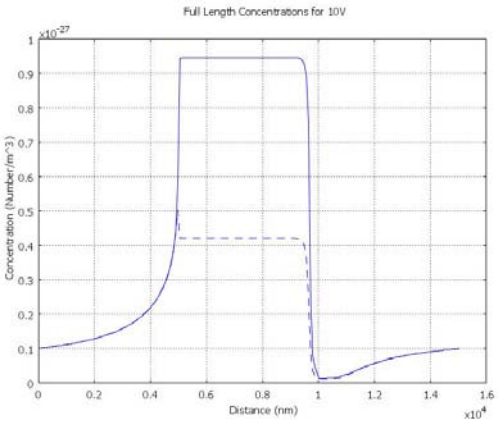

Figure 7. 10V applied. Cross sectional view of the ion concentrations. The left side is the grounded reservoir wall. The right side is the biased wall.

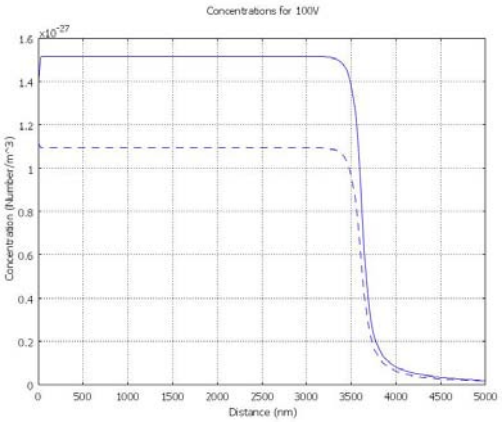

Figure 5. 100V applied across the nanochannel.

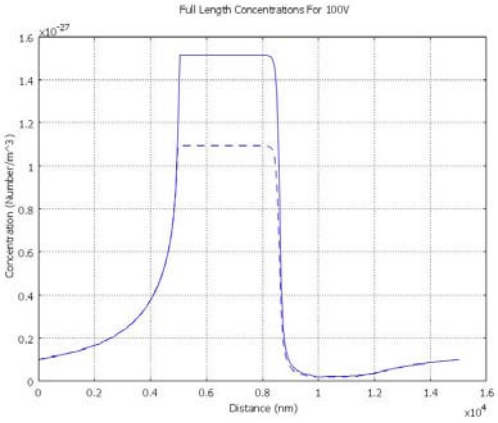

Figure 8. 100V applied. Cross sectional view of the ion concentrations. The left side is the grounded reservoir wall. The right side is the biased wall.

Outside of the nanochannel the ion concentrations eventually return to bulk values. However due to the wall charges as well as the applied voltage the ion concentrations have gradients well into the reservoirs. This can be seen by examining Figures 6-8 for each of the applied voltages. These figures are cross sections along the middle of the length of the nanochannel but extend to the walls of each reservoir.

We note here that smilar gradients are seen as well in the work of Rubinstein and Zaltzman [8]. In this work they analyze the ion concentrations outside of a permselective membrane as opposed to a physical channel. This implies that EOF is not included in their work as well.

An image of the potential plot for the case of 5V is included in Figure 9.

5. Conclusions

The depletion zones of ion concentration have implications related to the use of nanochannels in various "lab-on-a-chip" devices being explored recently. Although groups have explored the effect of the surface charge on the ionic current, few studies have considered the effects of the applied voltages on the structures of the concentration gradients.

The structures of the concentration gradients outside the nanochannels could be depend on time because ion species have different mobilities in the fluid. This would create very different distributions outside the nanochannel if one species of ions manages to get to the nanochannel faster than the other due to a higher mobility.

Future work on this project will focus on considering whether electro-neutrality is maintained overall within the channel. This has been a controversial topic as much previous work has assumed electro-neutrality while others state the condition is not held [9].

Modeling the site dissociation of molecules from the surfaces will more accurately portray the surface charge in future work [10]. In this scenario the surface charge will be dependent upon the local concentration of ions in the fluid. The surface charge in certain regimes can have important qualitative effects on the ion transport [11, 12].

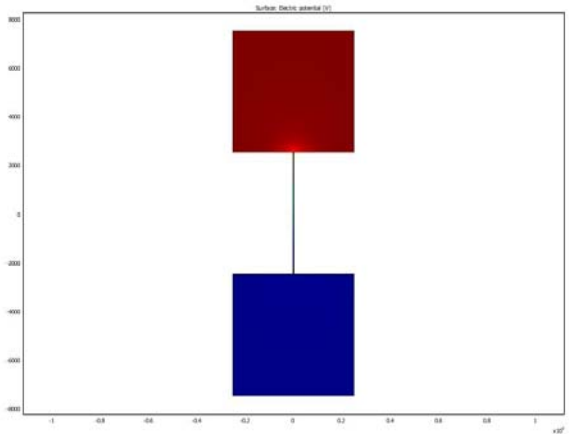

Figure 9. 5V case. Blue signifies low potential and red signifies high potential.

6. Acknowledgements

We gratefully acknowledge Phil Tabor for stylistic suggestions and funding from NSF Grant EPS-0554328, the WVNano Initiative, and the WVU Physics department.

7. References

1. Hunter R. J., *Zeta Potential in Colloid Science: Principles and Applications*, Academic, New York (1981)

2. Daiguji, H; Yang, P; Majumdar, A; Ion Transport in Nanofluidic Channels, *Nano Letters*, **Vol. 4**, No. 1, 137-142 (2004)

3. Zhang, Y.; Timperman, A. T. Integration of nanocapillary arrays into microfluidic devices for use as analyte concentrators, *Analyst* (Cambridge, United Kingdom) **2003**, *128*, 537-542.

4. Miller, S. A.; Kelly, K. C.; Timperman, A. T., Lab on a Chip **2008** *DOI*: 10.1039.

5. Tallarek, U; Holtzel, A; Ionic conductance of nanopores in microscale analysis systems: Where microfluidics meets nanofluidics, *J. Sep. Sci.*, **Vol. 30**, 1398-1419 (2007)

6. Masliyah, J; Bhattacharjee, S; *Electrokinetic and Colloid Transport Phenomena*, 105-171, John Wiley and Sons, New Jersey (2006)

7. Bath, B; Lee, R; White, H; Imaging Molecular Transport in Porous Membranes. Observation and Analysis of Electroosmotic Flow in Individual Pores Using the Scanning Electrochemical Microscope, *Anal. Chem.*, **Vol. 70**, 1047-1058 (1998)

8. Rubinstein, I; Zaltzman, B; Electro-osmotic Slip of the Second Kind And Instability in Concentration Polarization At Electrodialysis Membranes, *Mathematical Models and Methods in Applied Sciences*, **Vol. 11**, No. 2, 263-300 (2001)
9. Lee, M; Chan, K; Nicholson, D; Zara, S; Deviation from electroneutrality in cylindrical pores, *Chemical Physics Letters*, **Vol. 307**, 89-94 (1999)
10. Behrens, S; Grier, D; The Charge of Glass and Silica Surfaces, *Journal of Chemical Physics*, **Vol. 115**, Number 14 (2001)
11. Stein, D; Kruithof, M; Dekker, C; Surface-Charge-Governed Ion Transport in Nanofluidic Channels, *Physical Review Letters*, **Vol. 93**, Number 3 (2004)
12. Schooch, R; van Lintel, H; Renaud, P; Effect of the surface charge on ion transport through nanoslits, *Physics of Fluids*, **Vol. 17**, 100604 (2005)